

Electroproduction of Strangeness and Spectroscopy of Hypernuclei

M. Sotona

Nuclear Physics Institute, Prague

for core to core + SPHERE meeting, Prague 2010

Hypernuclear spectroscopy - hyperon - nucleon residual interaction, Λ behavior in nuclear environment (single particle energies, magnetic moment???),
.....

Hypernuclear spectroscopy on meson end photon beams

$$a + A \Rightarrow b + HN$$

$(K^-, \pi^-), (\pi^+, K^+), (K_{stopped}^-, \pi^-), (\gamma, K^+)$, reactions
Distorted Wave Impulse Approximation (DWIA) :

$$d\sigma \sim |T_{if}|^2 d\vec{p}_b d\vec{P}_{HN}$$

$$T_{if} \sim \sum_N \langle \Psi_b \Psi_{HN} | (b, \Lambda | t | a, N) | \Psi_a \Psi_A \rangle \quad (1)$$

Ψ_A, Ψ_{HN} - target (ground state) and hypernucleus many-particle wave functions (shell model)

Ψ_a, Ψ_b - meson wave functions (distorted waves, optical potential, eikonal approximation)

$(b, \Lambda | t | a, N)$ - t-matrix of elementary process or hadron current for reaction on individual nucleons

- Production cross section - strong dependence on momentum transferred to HN $q_{tr} = |\vec{p}_a - \vec{p}_b| \Rightarrow$ small pion, kaon scattering angles !!

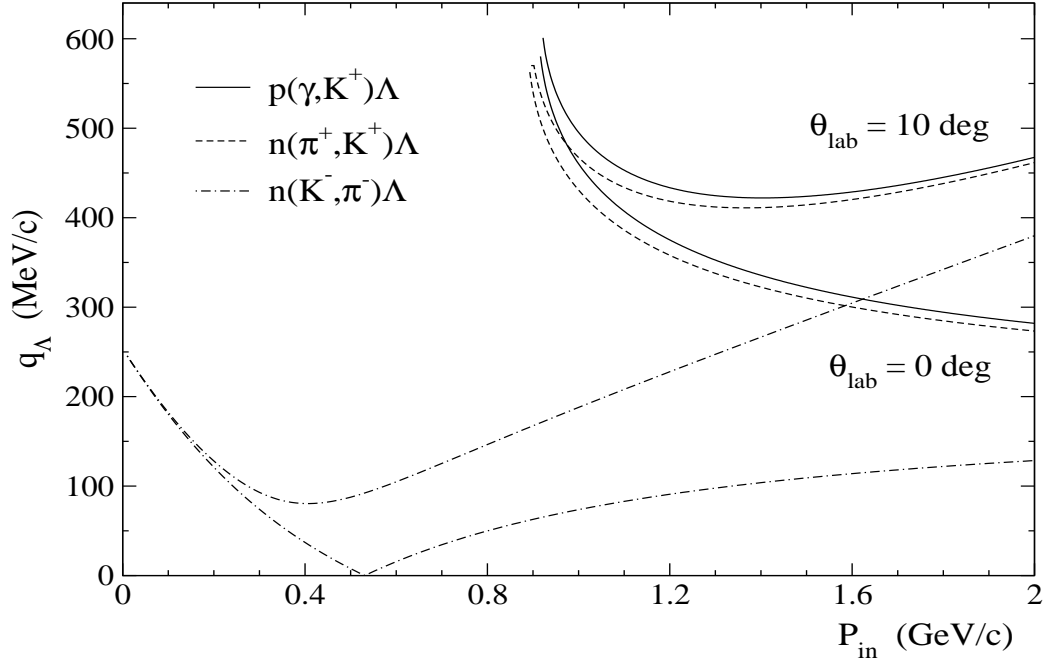


Figure 1: Momentum transfer in various strangeness production reactions.

- non-spin flip versus spin flip

K, π - pseudoscalar mesons $J^\pi = O^-$ - reaction amplitude

$$F = f(s, t) + ig(s, t)(\vec{\sigma} \cdot \vec{n}), \quad \vec{n} = \frac{\vec{p}_a \times \vec{p}_b}{|\vec{p}_a \times \vec{p}_b|}$$

non-spin-flip (f) (dominant at small scattering angles) and spin-flip (g) term.

photons (real or virtual)

$$J_{\text{lab}}^i = F_1(s, t)\sigma^i + iF_2(s, t)(\hat{q} \times \hat{p}_K)^i + F_3(s, t)(\vec{\sigma}\hat{q})\hat{p}_K^i + F_4(s, t)(\vec{\sigma}\hat{p}_K)\hat{p}_K^i + F_5(s, t)(\vec{\sigma}\hat{q})\hat{q}^i + F_6(s, t)(\vec{\sigma}\hat{p}_K)\hat{q}^i, \quad i = 0, \pm 1.$$

spin flip terms dominant even at small scattering angles)

(K^-, π^-) - $q_{tr} < k_F$, only $\Delta L = \Delta J = 0$, substitutional states

(π^+, K^+) - $q_{tr} > k_F$, $\Delta L = \Delta J = 1, 2$ HN

(γ, K^+) - $q_{tr} > k_F$, strong spin flip - $\Delta L = 1, 2$, $\Delta S = 1$, $\Delta J = 1, 2, 3$
states populated

Description of electro-production process

The kinematics of the electroproduction reaction

$$e(p_e) + p/A(p_p/p_A) \rightarrow e'(p'_e) + K^+(p_K) + \Lambda/HN(p_\Lambda/p_{HN})$$

on proton(p) or nuclear(A) target producing Λ hyperon or hypernucleus(HN) respectively is depicted in Fig.

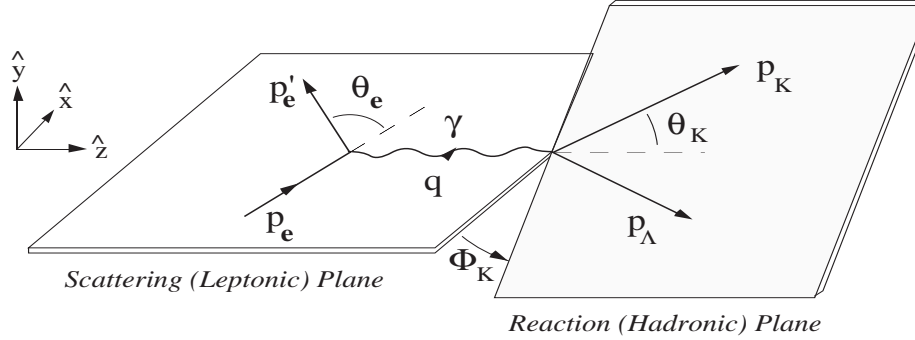


Figure 2: Kinematics of an electroproduction process.

To establish notation, the particle four-momenta are given in parentheses . Four-momentum transferred to the nucleon $q = \{\omega, \vec{q}\}$ (*virtual photon four-momentum*) is defined by $\omega = E_e - E'_e$, $\vec{q} = \vec{p}_e - \vec{p}'_e$. "Virtuality" of exchanged photon is determined by its (nonzero) four-momentum square q^2 . This photon is space-like ($q^2 < 0$) and for this reason the positive quantity $Q^2 = -q^2$ is usually used in the literature:

$$Q^2 = \vec{q}^2 - \omega^2 = 2(E_e E'_e - m_e^2 - |\vec{p}_e| |\vec{p}'_e| \cos \theta_e)$$

The triple differential cross section may then be expressed as a product of two terms, virtual photon flux Γ (determined only by electron kinematics) and the photoproduction cross section by virtual photons:

$$\frac{d^3\sigma}{dE'_e d\Omega'_e d\Omega_K} = \Gamma \frac{d\sigma}{d\Omega_K},$$

$$\frac{d\sigma}{d\Omega_K} = \frac{d\sigma_T}{d\Omega_K} + \epsilon_L \frac{d\sigma_L}{d\Omega_K} + \epsilon \frac{d\sigma_{TT}}{d\Omega_K} - \frac{Q^2}{\omega^2} l_{xz}^s \frac{d\sigma_{TL}}{d\Omega_K} - h \left\{ \frac{Q^2}{\omega^2} l_{yz}^a \frac{d\sigma_{TL'}}{d\Omega_K} - l_{xy}^a \frac{d\sigma_{TT'}}{d\Omega_K} \right\}.$$

Electroproduction on complex nuclear target

It is quite natural to suppose that in the one-photon-exchange approximation the transition amplitude of the electroproduction process *at complex nuclear target* can be written again as the invariant product of leptonic and hadronic currents mediated by the virtual photon propagator. Now, however, the hadron current is *many-particle operator* dependent on the internal structure of target nucleus and produced hypernucleus.

Distorted wave impulse approximation (DWIA) was successfully used to describe hypernuclear production in (K^-, π^-) , (π^+, K^+) and $(K_{stopped}^-, \pi^-)$ reactions. Rather high particle momenta ($|\vec{q}|, |\vec{p}_K| \simeq 1 \text{ GeV}$) involved in the electroproduction reaction justify an assumption that one can apply *DWIA* also in this case. The simple matrix element of single-particle hadron current in the transition matrix must be therefore substituted by the corresponding many-particle matrix element between the (nonrelativistic) nuclear and the hypernuclear wave functions

$$T_k^{if} = \langle \Psi_H | \sum_{j=1}^Z \chi_\gamma \chi_K^* J_k(p_\Lambda, p_K, p_p^j, q) | \Psi_A \rangle, \quad k = x, y, z.$$

The sum runs over the Z target protons and $\Psi_A(\Psi_H)$ is the many-particle (shell-model) wave function of target nucleus (hypernucleus). Virtual photon four-momentum $q = p_e - p'_e$, $p_p(p_\Lambda)$ are four-momenta of (bound) proton and hyperon. The quantity χ_γ is the virtual photon wave function (the product of the wave functions of incoming and outgoing electrons in the plane wave approximation - the Coulomb distortion is neglected for relativistic electrons). The kaon distorted wave χ_K is calculated in the optical potential model.

Important items of the calculation:

1. Ψ_A, Ψ_{HN} - target (ground state) and hypernucleus many-particle wave functions (shell model John Millener calculations)

Model space

- s_Λ states

$$|s^4 p^{n-4} JT, s_\Lambda J_{HN} T_{HN} \rangle$$

- p_Λ states

$$|s^4 p^{n-4} JT, p_\Lambda J_{HN} T_{HN} \rangle$$

$$|s^3 p^{n-3} JT, s_\Lambda J_{HN} T_{HN} \rangle$$

$$|s^4 p^{n-5} (sd) JT, s_\Lambda J_{HN} T_{HN} \rangle$$

- hyperon nucleon interaction

$$V_{\Lambda N}(r) = V_0(r) + V_\sigma(r) \vec{s}_N \vec{s}_\Lambda + V_\Lambda(r) \vec{l}_{N\Lambda} \vec{s}_\Lambda + V_N(r) \vec{l}_{N\Lambda} \vec{s}_N + V_T(r) S_{12}$$

The contribution of effective $\Lambda N - \Sigma N$ and $\Sigma N - \Sigma N$ interaction can be written in the same way

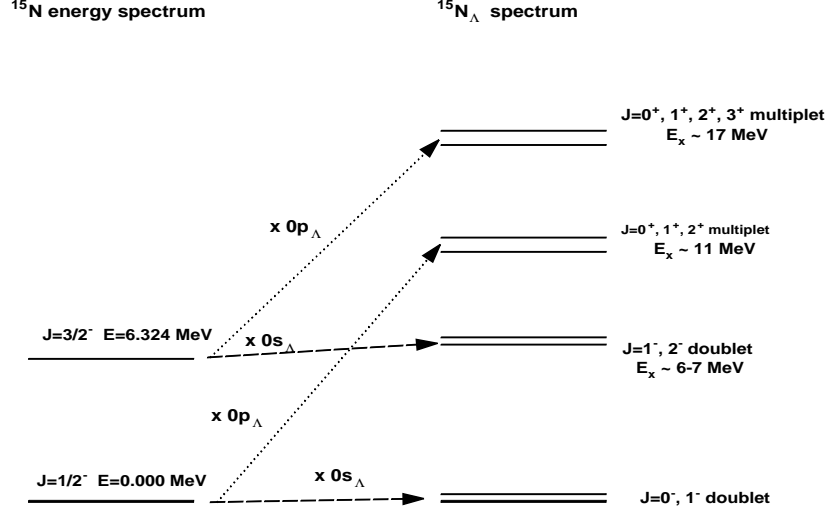


Figure 3: Weak coupling model and HN energy spectra

2. Ψ_a, Ψ_b - meson wave functions (distorted waves, optical potential, eikonal approximation)

First order optical potential

$$V_{opt} \sim \sigma_{tot} \left\{ i - \frac{Re f}{Im f} \right\} \rho(r)$$

σ_{tot} and ratio of real to imaginary part of forward scattering amplitude - from Martin or other parametrization of KN data.

3. model of hadron current for elementary process

$$J_{lab}^i = F_1(s, t) \sigma^i + i F_2(s, t) (\hat{q} \times \hat{p}_K)^i + F_3(s, t) (\vec{\sigma} \hat{q}) \hat{p}_K^i + F_4(s, t) (\vec{\sigma} \hat{p}_K) \hat{p}_K^i + F_5(s, t) (\vec{\sigma} \hat{q}) \hat{q}^i + F_6(s, t) (\vec{\sigma} \hat{p}_K) \hat{q}^i, \quad i = 0, \pm 1.$$

various hadrodynamics models fitted to all elementary process data.

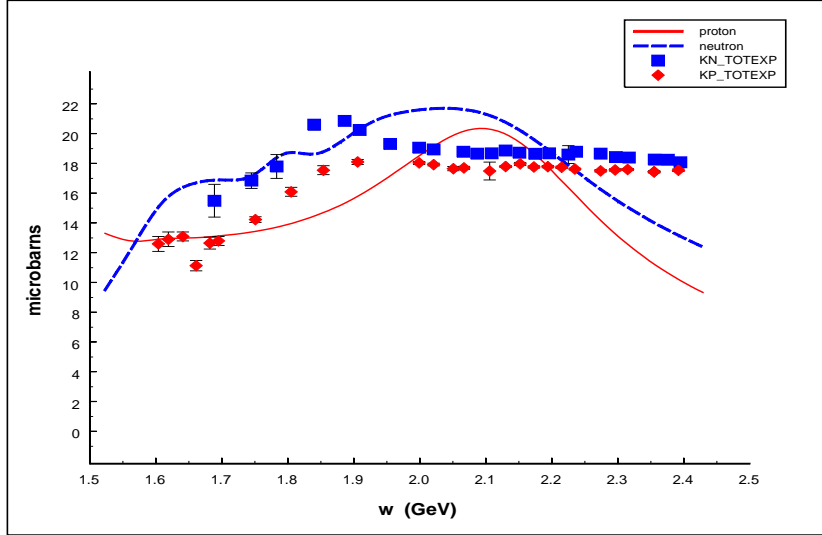


Figure 4: KN total cross section.

The cross section of elementary and many-particle process depend in principle on various combinations of six amplitudes involved and the models predicted the "same" cross sections and polarizations of elementary reaction can result in different predictions for the hypernuclear production

$^{12}\text{C}(e, e'K^+)^{12}\text{B}_\Lambda$ reaction, E89-009 Hall C experiment

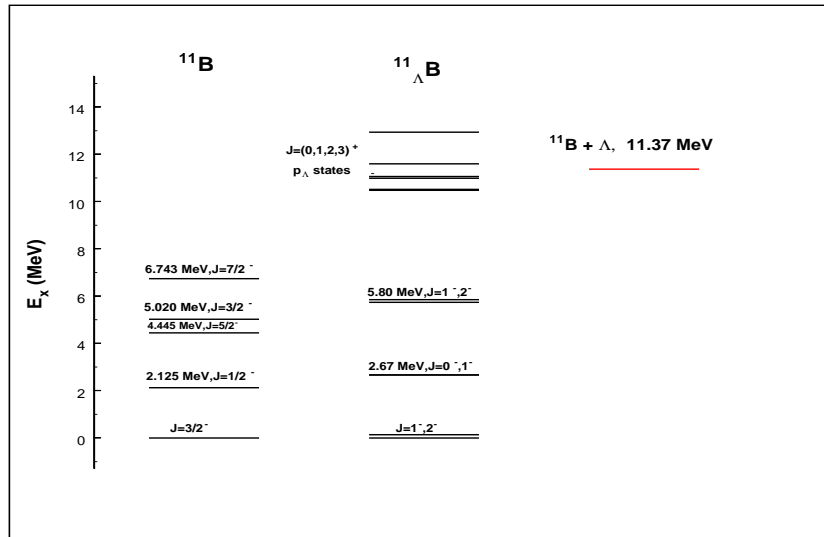


Figure 5:

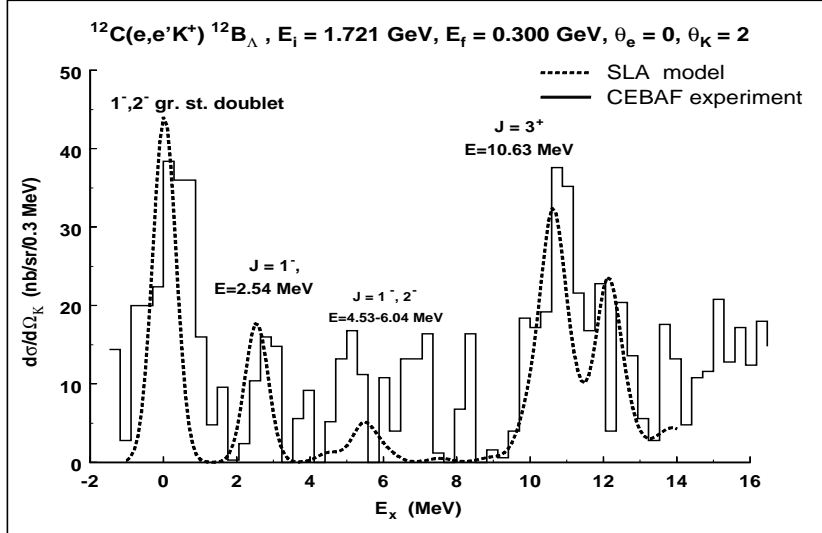


Figure 6: E 89-009 JLab experiment

Model dependence

Table 1: Differential cross section for $^{12}\text{C}(e, e'K^+)^{12}\text{B}_\Lambda$ reaction at kaon scattering angle $\Theta_{K\gamma} = 2$ and different electroproduction models

model	$E \simeq 0 \text{ MeV}$	$E = 2.54 \text{ MeV}$	$E \sim 5.5 \text{ MeV}$
AS2	123.7	49.4	16.9
WJC2	166.8	67.4	23.1
WJC3	107.6	42.9	14.8
WJC4	180.8	72.8	25.1
WJC1	143.5	57.2	19.7
AB1	138.9	55.5	19.1
SLA	140.7	56.9	19.5
KMAID	99.0	38.7	14.4
Exper.	$140 \pm 17 \pm 18$	$59 \pm 14 \pm 7$	$30 \pm 15 \pm 4$

We demonstrated that *Distorted Wave Impulse approximation* in standard form together with modern photoproduction models (Saclay - Lyon) is able to describe first hypernuclear electroproduction data taken on ^{12}C target reasonably well

E 94 - 107 Hall A experiment - ^{12}C target

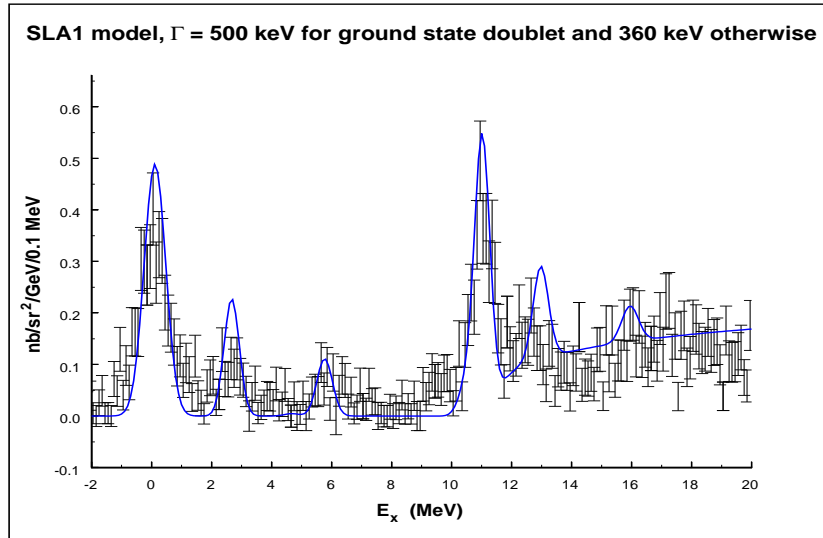


Figure 7: Hall A experiment and theoretical predictions

What we can learn from the comparison of $^{12}\text{C}_\Lambda$ and $^{12}\text{B}_\Lambda$?

Λ binding energy $B_\Lambda = 10.8 \text{ MeV} (^{12}\text{C}_\Lambda)$, $11.37 \text{ MeV} (^{12}\text{B}_\Lambda)$ - *charge symmetry breaking in $\Lambda - N$ interaction or some problem with photoemulsion B_Λ value for $^{12}\text{C}_\Lambda$??*

E 94 - 107 Hall A experiment - ^{16}O target

Schematic picture of expected energy spectra:

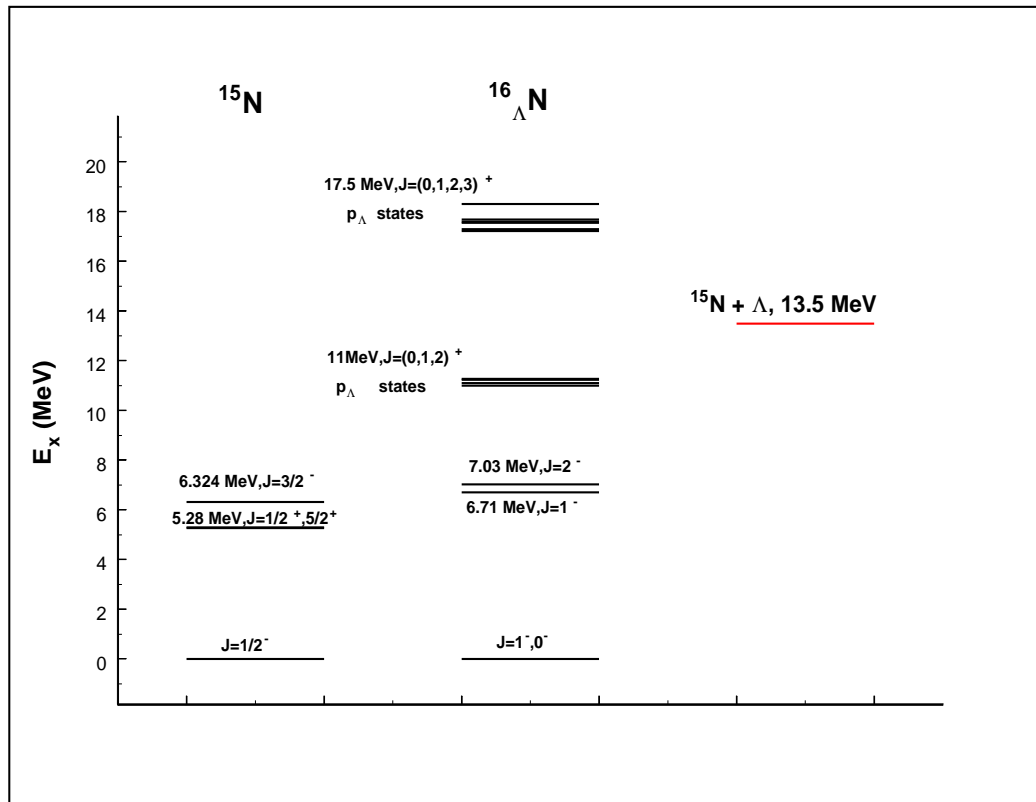


Figure 8:

Contribution of individual levels

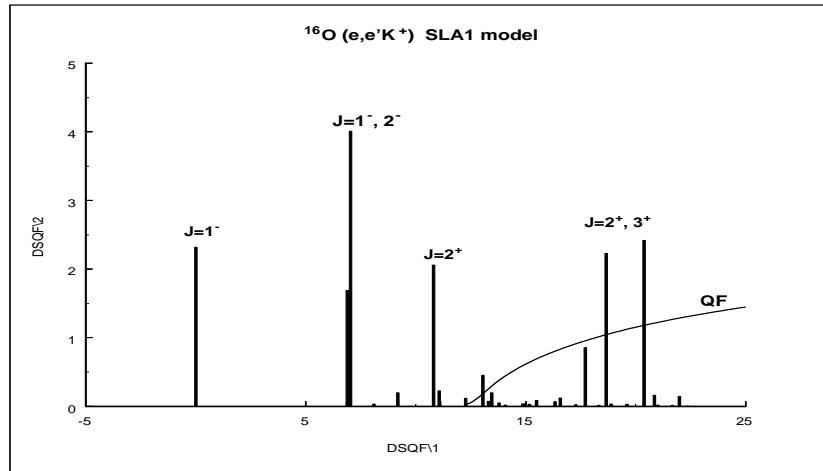


Figure 9: Contribution of individual HN levels

Results of Hall A experiment

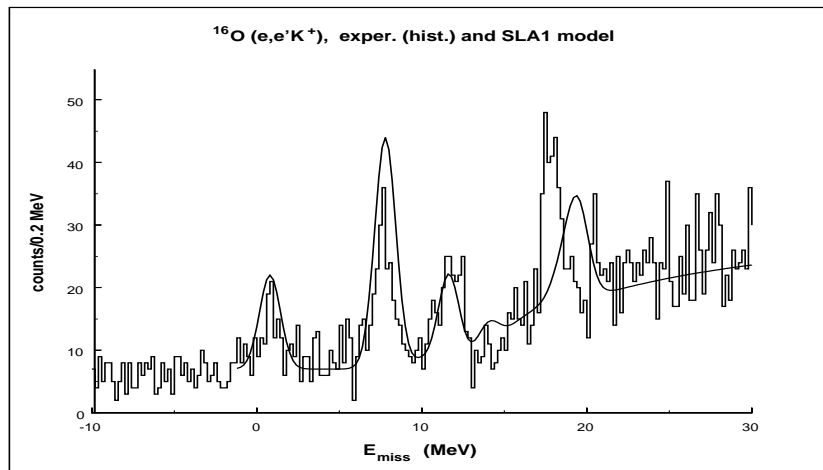


Figure 10:

E 94 - 107 Hall A experiment - ${}^9\text{Be}$ target

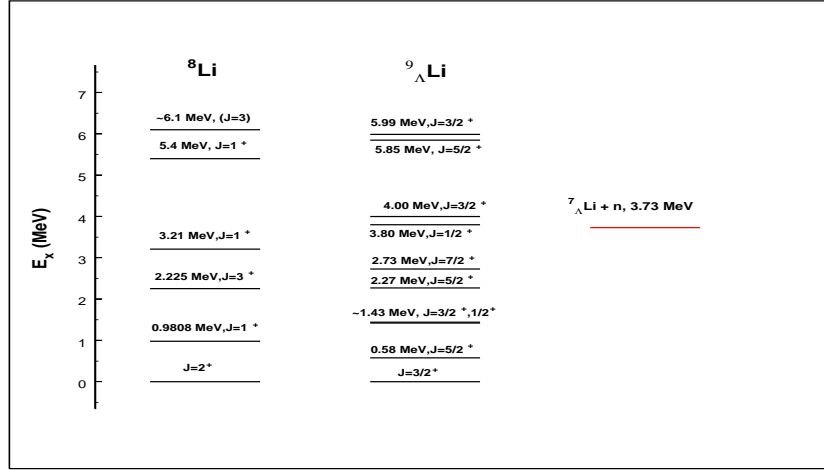


Figure 11: Calculated energy spectra - John Millener

In Fig.1 you can see experimental energy spectrum of "underlying" core nucleus ${}^8\text{Li}$ (left side) and that of ${}^9_{\Lambda}\text{Li}$ hypernucleus HN states) as calculated by John Millener. One can see again typical pattern of hypernuclear doublets :

1. doublet of HN states $J = 3^+/5/2^+$ at excitation energies $E = 0.00/0.58\text{MeV}$ corresponding to s_{Λ} coupled to ${}^8\text{Li}$, $J = 2^+$ ground state
2. practically degenerate doublet of HN states $J = 3/2^+/1/2^+$ at $E_x = 1.42/1.44\text{MeV}$ generated from $J = 1^+$, $E = 0.9808\text{MeV}$ state of ${}^8\text{Li}$ core
3. third doublet of $J = 5/2^+/7/2^+$ states at $E_x = 2.27/2.73\text{MeV}$ generated from $J = 3^+$, $E = 2.225\text{MeV}$ state of ${}^8\text{Li}$ core
4. and the last one $J = 1/2^+/3/2^+$ at $E_x = 3.80/4.00\text{MeV}$ generated from $J = 1^+$, $E = 3.21\text{MeV}$ state of ${}^8\text{Li}$ core

Then there is a gap $E_x = 3.21 - 5.4\text{MeV}$ in ${}^8\text{Li}$ energy spectrum but John calculation predict some HN states in this energy region. I can see following reason:

1. energy spectrum of ${}^8\text{Li}$ nucleus is not known too well. There could be some missing states hardly produced in some standard nuclear reactions used in spectroscopy

2. ${}^8\text{Li}$ is unstable it decays by β emission. In addition, the lowest threshold for strong ${}^8\text{Li} \Rightarrow {}^7\text{Li} + n$ decay is as low as $E_{\text{threshold}} = 2.032\text{MeV}$ and all higher states are resonances - it is a question if such states can be described reasonably by shell model
3. as we shall see in next Sect. also HN states corresponding to these higher states of ${}^8\text{Li}$ are only weakly populated and they lie in HN continuum - they should be hardly recognizable in our spectrum

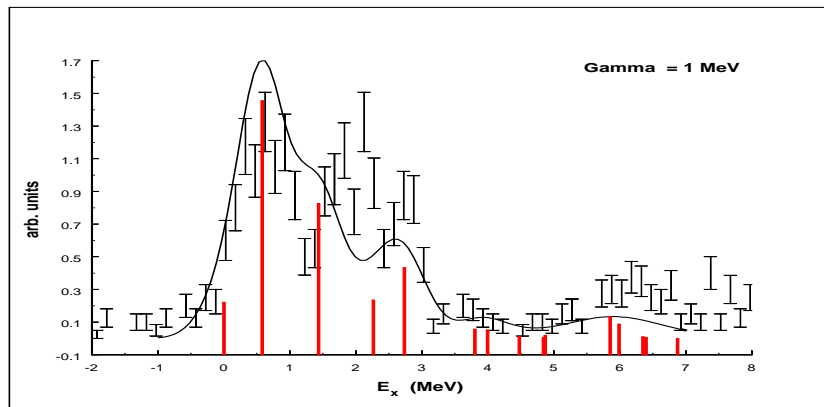


Figure 12: Calculated versus experimental cross section

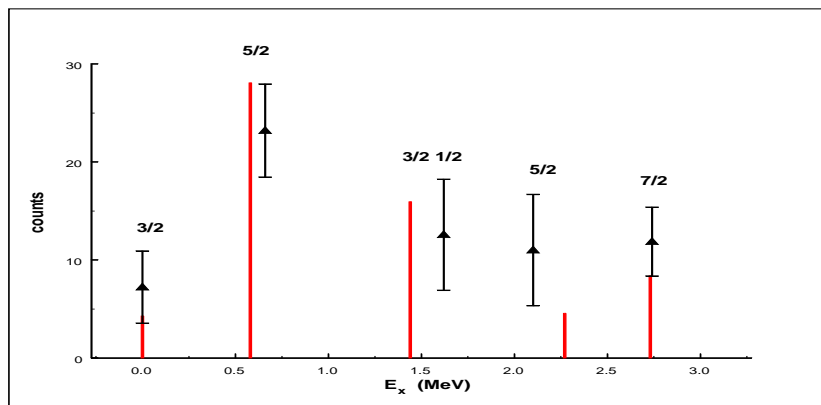


Figure 13: Comparison of theoretical predictions and experimental data.